An ITPA joint experiment to study runaway electron generation and suppressiona)

R. S. Granetz, B. Esposito, J. H. Kim, R. Koslowski, M. Lehnen, J. R. Martin-Solis, C. Paz-Soldan, T. Rhee, J. C. Wesley, L. Zeng, and ITPA MHD Group

Citation: Physics of Plasmas (1994-present) **21**, 072506 (2014); doi: 10.1063/1.4886802
View online: http://dx.doi.org/10.1063/1.4886802
View Table of Contents: http://scitation.aip.org/content/aip/journal/pop/21/7?ver=pdfcov
Published by the AIP Publishing

An ITPA joint experiment to study runaway electron generation and suppression[a)]

R. S. Granetz,[1,b),c)] B. Esposito,[2] J. H. Kim,[3,4] R. Koslowski,[5] M. Lehnen,[6] J. R. Martin-Solis,[7] C. Paz-Soldan,[8] T. Rhee,[3] J. C. Wesley,[9] L. Zeng,[10] and ITPA MHD Group

[1]*MIT Plasma Science and Fusion Center, Cambridge, Massachusetts 02139, USA*
[2]*ENEA Unità, Tecnica Fusione, C.R. Frascati, Via E. Fermi 45, 00044-Frascati, Roma, Italy*
[3]*National Fusion Research Institute, Daejeon 305-806, Korea*
[4]*Department of Nuclear Fusion and Plasma Science, University of Science and Technology, Daejeon 305-350, Korea*
[5]*Forschungszentrum Jülich GmbH, Institut für Energie- und Klimaforschung – Plasmaphysik, 52425 Jülich, Germany*
[6]*ITER Organization, Route de Vinon sur Verdon, 13115 St Paul Lez Durance, France*
[7]*Universidad Carlos III de Madrid, Avenida de la Universidad 30, 28911-Madrid, Spain*
[8]*Oak Ridge Institute for Science and Education (ORISE), Oak Ridge Tennessee 37831, USA*
[9]*General Atomics, PO Box 85608, San Diego, California 92186-5608, USA*
[10]*Institute of Plasma Physics, Chinese Academy of Sciences, PO Box 1126, Hefei, Anhui 230031, China*

(Received 4 April 2014; accepted 9 June 2014; published online 11 July 2014)

Recent results from an ITPA joint experiment to study the onset, growth, and decay of relativistic electrons (REs) indicate that loss mechanisms other than collisional damping may play a dominant role in the dynamics of the RE population, even during the quiescent I_p flattop. Understanding the physics of RE growth and mitigation is motivated by the theoretical prediction that disruptions of full-current (15 MA) ITER discharges could generate up to 10 MA of REs with 10–20 MeV energies. The ITPA MHD group is conducting a joint experiment to measure the RE detection threshold conditions on a number of tokamaks under quasi-steady-state conditions in which V_{loop}, n_e, and REs can be well-diagnosed and compared to collisional theory. Data from DIII-D, C-Mod, FTU, KSTAR, and TEXTOR have been obtained so far, and the consensus to date is that the threshold E-field is significantly higher than predicted by relativistic collisional theory, or conversely, the density required to damp REs is significantly less than predicted, which could have significant implications for RE mitigation on ITER. © *2014 AIP Publishing LLC*.
[http://dx.doi.org/10.1063/1.4886802]

I. INTRODUCTION

Theoretical calculations predict that disruptions of full-current (15 MA) discharges in ITER are likely to generate up to 10 MA of current carried by runaway electrons (RE), having relativistic energies of 10–20 MeV.[1] If these runaways hit the blanket modules or the divertor in a localized area over a short timescale, significant damage will occur. Therefore, it is necessary to mitigate the runaways before or during their formation, and a number of different physical processes have been suggested to accomplish this. Electron energy loss via Coulomb collisions, i.e., collisional drag, is probably the best understood of these from a physics standpoint and is therefore considered a candidate for RE mitigation on ITER. However, this requires an electron density of order $4 \times 10^{22}\,m^{-3}$ (the "Rosenbluth" density), *assuming there are no other RE loss mechanisms that come into play*. Fueling to this density by injection of noble gas on the required timescale of ~10–20 ms has proven to be exceedingly difficult in present-day tokamaks, and it would have significant consequences for the ITER tritium recycling plant and the NBI cryopumps, and possibly result in a current decay that is faster than permissible (36 ms for a full-current disruption). Fueling to this extremely high density would not be required if it could be reliably shown that other RE loss mechanisms in addition to collisional damping commonly exist on tokamaks, both during the flattop and during disruptions.

This paper briefly reviews the basic physics of primary (Dreicer) runaway electron generation and the critical electric field. This is followed by a description of the ITPA joint study of runaway onset conditions during quiescent, flattop conditions. Results from the participating tokamaks are presented, and important caveats are discussed. An alternative technique to determine the RE threshold conditions by looking at the transition between RE growth and decay is presented. Finally, the implications for ITER are discussed.

II. PRIMARY (DREICER) RUNAWAY ELECTRON GENERATION

In tokamaks, a toroidal electric field is applied to drive plasma current ($E = V_{loop}/2\pi R$). This E-field exerts a force $F_E = qE$, on the free electrons in the plasma, which in principle can accelerate them. (The E-field exerts a force on the ions as well, but their relatively high mass essentially

[a)]Paper BI2 3, Bull. Am. Phys. Soc. **58**, 22 (2013).
[b)]Invited speaker.
[c)]Author to whom correspondence should be addressed. Electronic mail: granetz@mit.edu.

excludes them from the problem of interest in this paper.) However, frictional drag is effectively generated by Coulomb collisions with the background distribution of electrons in the plasma, and this frictional drag force opposes the acceleration by the E-field. As long as this collisional drag force on an electron is of greater magnitude than the force due to the toroidal E-field, the electron will not be accelerated and will remain within the thermal distribution. The collisional drag force on an electron is expressed in terms of a collisionality, ν, defined by the following expression:

$$F_{\mathrm{coll}} = m\frac{d\mathrm{v}}{dt} = -m\nu\mathrm{v}. \tag{1}$$

The collisionality for an electron of velocity, v, on a background Maxwellian distribution of electrons with density, n, derived from classical electrodynamics, is:

$$\nu(\mathrm{v}) = \frac{q^4 n \ln\Lambda}{4\pi\varepsilon_0^2 m^2 \mathrm{v}^3}. \tag{2}$$

Note that the collisionality decreases like v^3, so fast electrons experience less collisional drag than thermal electrons. (Fast electrons also collide with the ion background but due to the large mass ratio, these collisions do not effectively reduce the electron speed, and therefore have a negligible contribution to the drag force.) In order for an electron to accelerate, the electric field force must be greater than the collisional damping force:

$$F_{\mathrm{E}} > F_{\mathrm{coll}}, \tag{3}$$

in which case, an electron will gain energy indefinitely, i.e., runaway, *if there are no other loss mechanisms*. Combining the above equations gives a threshold condition for runaway generation:

$$E > \frac{n q^3 \ln\Lambda}{4\pi\varepsilon_0^2 m \mathrm{v}^2}. \tag{4}$$

This condition, derived from classical electrodynamics, implies that no matter how small the applied E-field is, electrons with a sufficiently high velocity can runaway. However, special relativity sets an upper limit on the electron velocity, $\mathrm{v} \leq \mathrm{c}$, and therefore a lower limit, i.e., a minimum E-field required to generate any runaways. A full relativistic treatment[2] gives:

$$E_{\mathrm{crit}} = \frac{n q^3 \ln\Lambda}{4\pi\varepsilon_0^2 m c^2}. \tag{5}$$

For applied electric fields just above the E_{crit} threshold, only electrons in the tail of the velocity distribution can runaway, as shown schematically in Figures 1(a) and 1(b). In the Dreicer[3] model, the tail electrons that runaway will have diminishing interaction with the background distribution, since their collisionality continues to decrease as they continue to be accelerated by the electric field. Conceptually, they form their own distinct population which is independent of the plasma, but they leave behind a deficit in the velocity distribution, which is filled in by diffusion in velocity space from the background distribution. These replacement electrons will also accelerate and run away, setting up a continuous process of velocity space diffusion and runaway acceleration. Therefore, the growth rate of the runaway electron population due to this primary production mechanism is set by the fill-in rate, as given by Eq. (63) in Ref. 2. The RE growth by this primary mechanism is therefore linear, not exponential. There is also a secondary (avalanche) RE generation mechanism which will be discussed later.

In the expression for E_{crit} (Eq. (5)), all parameters except density, n, and the Coulomb logarithm, ln Λ, are constants of nature. The Coulomb logarithm, ln Λ, varies relatively little for the plasmas of interest, and therefore is nearly a constant. Assuming a representative value of 15 for ln Λ, the expression for E_{crit} becomes:

$$E_{\mathrm{crit}} \cong 0.08 n_{20}, \tag{6}$$

where n_{20} is the plasma electron density in units of $10^{20}\,\mathrm{m}^{-3}$. This simple criterion is conceptually illustrated in Figure 2, which shows the RE population (color scale) as a function of electron density and E-field. The threshold condition, Eq. (6), is simply a line in this space. For sufficiently low E-fields and/or sufficiently high densities, no runaways can be generated. Conversely, for sufficiently high E-fields and/or sufficiently low densities, runaways can be generated *if there are no other RE loss mechanisms*. During the current quench of a 15 MA disruption on ITER, it is estimated that the toroidal electric field could jump to 38 V/m.[4] Using Eq. (6), an electron density of $4\text{-}5 \times 10^{22}\,\mathrm{m}^{-3}$ would be required to remain below the Connor-Hastie RE threshold in order to prevent runaways in ITER, and as mentioned in the introduction, achieving this density is quite problematic. But Eq. (6) very likely underestimates the threshold E-field (or conversely, overestimates the threshold density) because the Dreicer and Connor-Hastie models do not incorporate some of the basic features of magnetic confinement devices that could give rise to additional RE losses. In particular, those theoretical derivations do not have any magnetic field, so no

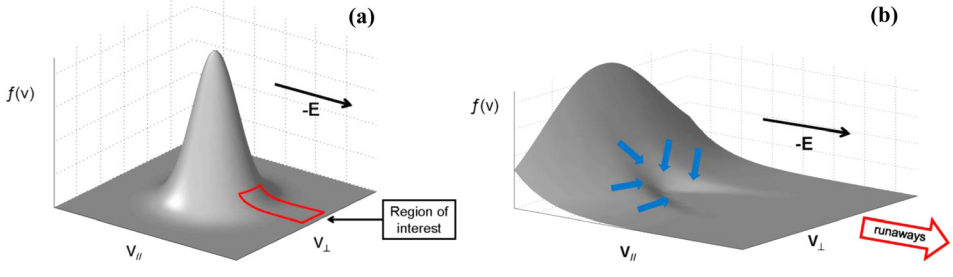

FIG. 1. (a) For E just above E_{crit}, only the tail of the electron distribution can run away (region shown schematically by red box). (b) The growth rate of the runaway population is set by the rate at which electrons from the thermal distribution continuously fill in the deficit left by the electrons that continuously runaway (blue arrows).

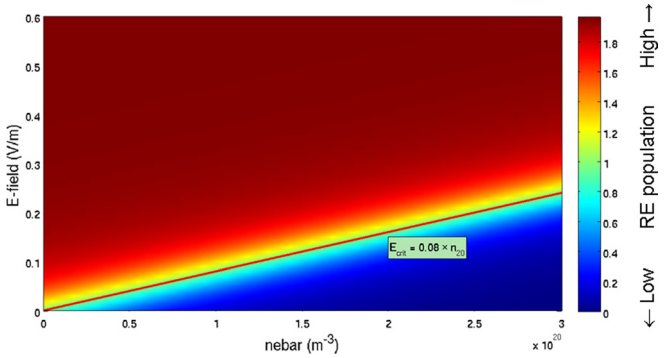

FIG. 2. Conceptual illustration of RE threshold condition as a function of *E*-field and density. The color scale represents RE population. The red line is the Connor-Hastie E_{crit}.

synchrotron emission losses from Larmor motion is included. They do not have any toroidicity, and therefore have no synchrotron losses from toroidal motion, nor particle losses due to drift orbit excursions. Since they do not have a magnetic field, they also don't have *B*-field fluctuations, which might cause stochastic RE particle loss. And they don't consider beam instabilities, which might cause scattering in velocity space, leading to enhanced synchrotron emission loss. Given that tokamaks have the aforementioned features, it should not be surprising if empirically determined RE thresholds were found *not* to agree with Eq. (6). Indeed, there has long been anecdotal evidence that tokamaks can run above the Connor-Hastie threshold condition without having runaways. A documented example of this on FTU is given in Ref. 5. Given the necessity of mitigating disruption runaways in ITER, it is important to experimentally determine on a broad set of tokamaks if the Connor-Hastie threshold is relevant.

III. ITPA JOINT EXPERIMENT

The International Tokamak Physics Activity (ITPA) is coordinated by the ITER organization to facilitate experiments and data analyses on present fusion devices in order to provide guidance for ITER designs and planning. There is an ITPA MHD group, which incorporates a number of topical areas, including disruptions and runaway electrons. Under certain circumstances, ITPA groups have carried out experiments jointly on several devices to help elucidate key physics issues. The question of whether or not other RE loss mechanisms in addition to collisional damping commonly exist in tokamaks is ideally suited to investigation via a joint ITPA experiment, as long as well-defined experimental guidelines can be delineated. A proposal to do this was developed, refined, and formally initiated, with researchers representing a number of machines agreeing to participate, either by running dedicated experiments, or by analyzing suitable existing data. The basic plan, as devised by the group, is to map out the threshold conditions for the onset of runaway electrons in terms of the two parameters, density and *E*-field, and compare the findings to the theoretical threshold shown in Fig. 2. Although the motivation for this study is runaways during disruptions, in order to make the best comparison to theory, it is desirable to obtain the threshold data under well-controlled, reproducible, well-diagnosed conditions, i.e., *not during disruptions*. For this reason, the guidelines for the joint experiment specify that the measurements be made during the flattop portion of the discharge in each machine, when plasma parameters are essentially constant, and the plasma is in a relatively quiescent state. In addition, in order to avoid complications due to non-Maxwellian electron distributions, discharges with lower hybrid or electron cyclotron waves are excluded.

A. Experimental measurements of RE onset threshold

Dedicated experiments to measure the density and *E*-field have been carried out on three tokamaks so far: TEXTOR, FTU, and DIII-D. On two other tokamaks, Alcator C-Mod and KSTAR, previously existing data has been analyzed to determine RE detection threshold values. This study in these small- to medium-size devices covers a range of plasma parameters, as shown in the Table I.

The TEXTOR experiment was done by running a series of discharges, all with identical plasma current, *B*-field, shape, etc. During the flattop of each discharge, the electron density was held very constant. The density was reduced on a shot-to-shot basis until the signal on an infrared camera started to increase, indicating the creation of a measurable population of runaway electrons. Figure 3 shows a set of three discharges with slightly different densities during the flattop (top panel). The middle panel shows a signal from an infrared (IR) camera which detects synchrotron emission from relativistic runaways, and the RE onset can clearly be discerned at $t \sim 2.6$ s on the shot with the lowest density (in red). The loop voltage traces are shown in the lower panel. Due the steady-state quiescent conditions, which are held for 4 s on each discharge, the density and *E*-field at the RE onset are accurately measurable, and found to be $n = 0.07 \times 10^{20}\,\mathrm{m}^{-3}$ and $E = 0.066$ V/m, which is well above the Connor-Hastie threshold, as shown in Figure 8. These onset parameters on TEXTOR are found to be very reproducible.

Data from FTU, which also performed dedicated experiments, is shown in Figure 4. Unlike in TEXTOR, the RE onset was obtained by slowly letting the density ramp down during the current flattop of each discharge, instead of shot-to-shot. FTU uses an NE213 scintillator detector to measure hard x-rays generated by runaways. However, the NE213 scintillator is also sensitive to fusion neutrons, which are present as well, and which are independently measured by calibrated BF_3 counters. Therefore, the RE onset is delineated by the divergence of these two signals at $t \approx 0.8$ s.

TABLE I. Plasma parameters for devices in this study.

Device	I_p (MA)	B_T (T)	$T_e(0)$ (keV)	Z_{eff}	Configuration
TEXTOR	0.3	2.4	2	-	Limited, circular
FTU	0.5	6	3.6	6	Limited, circular
DIII-D	0.8	1.5	0.6–1.9	1.3–2.5	Diverted, elongated
C-MOD	0.55–1.0	5.4	2.5–4	3.7–7	Diverted, elongated
KSTAR	0.4–0.6	1.96	2–3	2.0–2.5	Diverted, elongated

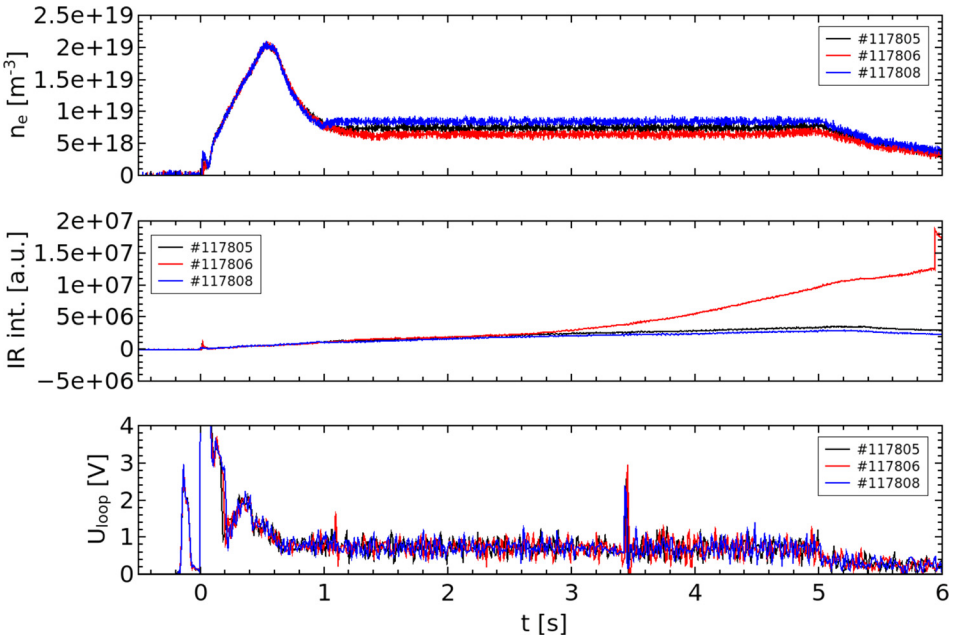

FIG. 3. Data from TEXTOR showing density (top panel), IR signal from runaway synchrotron emission (middle panel), and loop voltage (lower panel) for a series of 3 discharges. The lowest density shot (red) shows the onset of runaways at t ≅ 2.6 s.

At this time, the relevant onset parameters are $n = 0.25 \times 10^{20}\,\mathrm{m}^{-3}$ and $E = 0.17\,\mathrm{V/m}$, as shown with the point labeled "FTU" in Figure 8.

On DIII-D, as with FTU, the RE onset was triggered by slowly letting the density decay during the I_p flattop of the discharges and observing the sudden increase in hard x-ray flux measured by a plastic scintillator. Figure 5 shows the densities (top panel) and hard x-ray signals (middle panel) from four representative discharges. (Note that the HXR is shown on a log scale.) The HXR onset times are indicated with vertical dotted lines. Densities and E-fields at the HXR onsets on a number of shots are shown in Table II and plotted in Figure 8. The onset densities are near the low end of the DIII-D operating range, and special care has been taken to avoid locked modes that are sometimes present under these conditions, thus avoiding any possible effect they may have on the RE threshold. The standard deviation of the threshold condition, E/n, is only 2.7%, demonstrating the excellent reproducibility of the measurements. A much more detailed account of the DIII-D experiments in support of this ITPA joint study is presented in Ref. 6. It includes measurements of the RE growth and decay rates, which will be discussed in Sec. III D, as well as calculations of the expected RE population vs time based on collisional theory, and information on the measured RE emission spectra and spatial pattern, and internal magnetic fluctuation levels during the ohmic flattop, which are outside the scope of this work.

Dedicated run time was not available on Alcator C-Mod nor KSTAR, so existing data from non-dedicated runs have

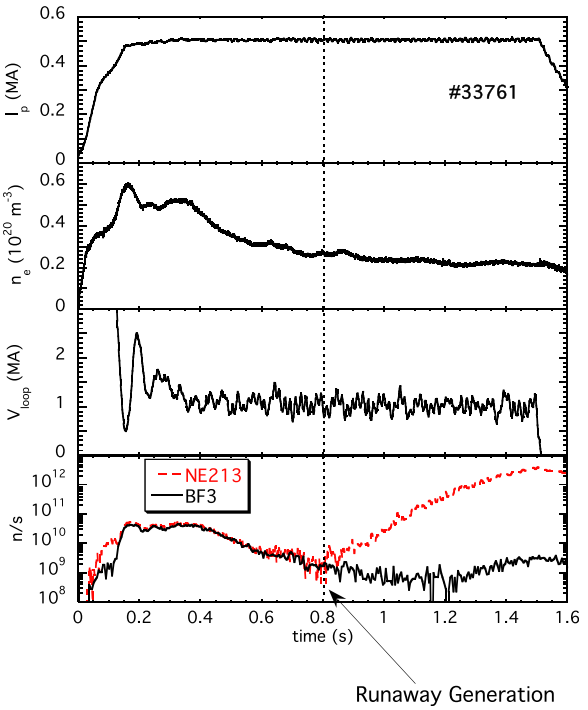

FIG. 4. Data from FTU showing I_p, n_e, V_{loop}, and hard x-ray signals (top to bottom, respectively). The RE onset is denoted at t ≈ 0.8 s.

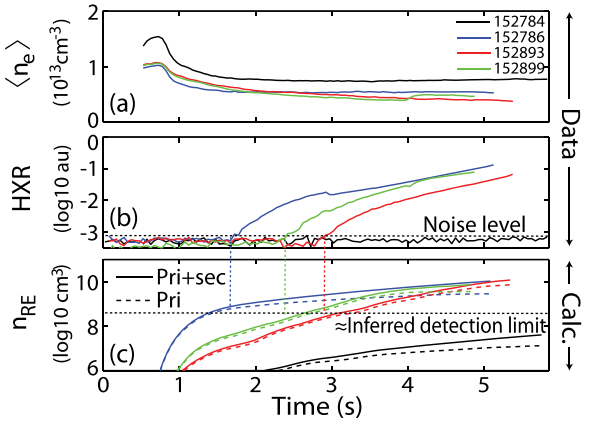

FIG. 5. Data from DIII-D showing density and hard x-ray signals from a series of discharges. Runaways are triggered during the I_p flattops by letting the density decay. The RE detection onset times are indicated by the vertical dotted lines. (Adapted with permission from Ref. 6; copyright 2014 American Institute of Physics.)

TABLE II. Measured E-fields and densities at RE onset for several of the DIII-D shots in this study. The threshold condition, E/n, shows excellent reproducibility.

Shot	E (V/m)	n_e (10^{20} m^{-3})
152 892	0.052	0.046
152 893	0.055	0.050
152 897	0.053	0.048
152 899	0.054	0.047
152 786	0.060	0.056

been analyzed. On C-Mod, a dataset has been compiled from time slices of the loop voltage, density, and hard x-ray signals during the flattops of all non-disruptive (during the I_p flattop), non-LHCD discharges from the most recent 3 years of plasma operation. Over 150 000 samples are in the dataset, spanning densities over the range $0.3–6 \times 10^{20}$ m^{-3}. Appreciable runaways are observed only at the very low end of the C-Mod density range, as can be seen in Figure 6. The runaway regime is delineated by a line at about $5 \times E_{crit}$, which essentially defines the threshold condition on C-Mod. Note that there are many points above the empirical threshold that do not have runaways (light gray), perhaps hinting that some other parameter(s) might be involved in the RE physics. A similar study has been done on a dataset from the KSTAR 2012 campaign, and a similar threshold found, as shown in Figure 7.

The RE onset data from the dedicated runs on DIII-D, FTU, and TEXTOR, and the analysis of non-dedicated runs on C-Mod and KSTAR, are compiled together in Figure 8, along with the theoretical $E_{crit}(n)$ threshold from Connor-Hastie (solid line), and dashed lines at $5 \times E_{crit}$ and $10 \times E_{crit}$. The measured threshold E-fields on TEXTOR and DIII-D are a factor of 10-12 times above E_{crit}, 8.5 times higher on FTU, and 4.5–5 times higher on C-Mod and KSTAR. Conversely, the threshold densities are at least$\sim$5 times less than predicted by the collisional theory for a given electric field. The well-diagnosed and reproducible results from this set of tokamaks suggest that there are other RE loss mechanisms in addition to collisional drag, even during quiescent, flattop conditions, and that these additional loss mechanisms dominate over collisional damping.

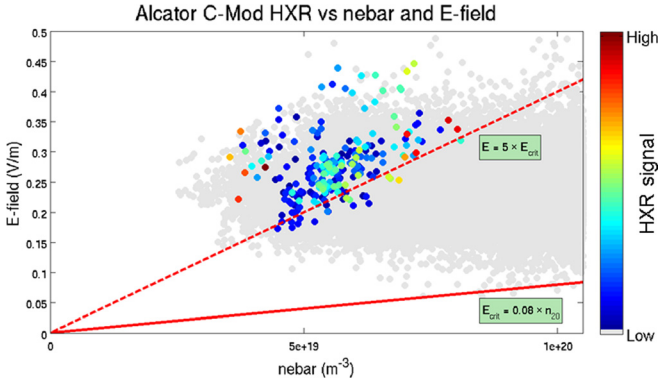

FIG. 6. RE data from Alcator C-Mod, based on analysis of a large set of non-disruptive discharges. The points in the plot correspond to discrete times during the flattop. Runaways (indicated by finite HXR signal) only appear at the very low end of the C-Mod density range, at E-fields that are $\gtrsim 5 \times E_{crit}$.

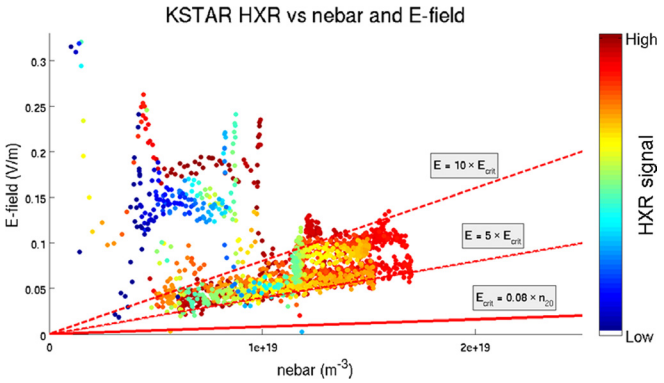

FIG. 7. RE data from KSTAR, based on analysis of a large set of non-disruptive discharges. The points in the plot correspond to discrete times during the flattop. Runaways only appear at E-fields that are $\gtrsim 5 \times E_{crit}$.

B. Caveat on the RE onset method

There are important caveats about determining the runaway threshold conditions based on observations of the onset of runaways. RE detectors (hard x-ray or synchrotron) have finite sensitivities and finite noise levels, which translate into minimum detectable levels of runaways. In a Maxwellian distribution of a few keV, with electron densities and E-fields representative of this ITPA joint experiment, the initial number of runaways is well below detectable limits. Therefore, once the threshold condition has been surpassed, the growth of a runaway population to measurable levels requires a finite amount of time. If the relevant plasma parameters (n_e, V_{loop}, T_e, Z_{eff}) change during this growth period, the determination of threshold conditions will depend on the detection threshold, rather than the RE growth threshold, which could lead to inaccurate results. For example, measurements of T_e(t), and Z_{eff}(t) on DIII-D make it possible to calculate the expected RE density vs time based on collisional theory,[6] as shown in the bottom panel of Figure 5. Direct comparison with the measured HXR in the middle panel does not show agreement, which we have construed as evidence for additional loss mechanisms. However, if a detection limit is inferred at the level shown by the horizontal dotted line, then collisional theory and experiment agree fairly well, and no additional loss mechanisms are warranted. Thus, the absolute sensitivities of the RE detectors matter. However, none of the RE detectors on the machines in this study are absolutely calibrated, and it is not clear if such absolute calibrations could feasibly be done. In principle, therefore, the accuracy of determining the threshold conditions from the observed RE onsets is difficult to assess, although the excellent reproducibility of the measurements does lend some legitimacy to the results. Because of these caveats, an alternate method of comparing empirical RE thresholds to collisional theory by focusing on growth and decay rates is described in the next sections.

C. Secondary (avalanche) RE production mechanism

Once a population of runaway electrons is established by the primary production mechanism, a secondary production mechanism, known as knock-on or avalanching, can

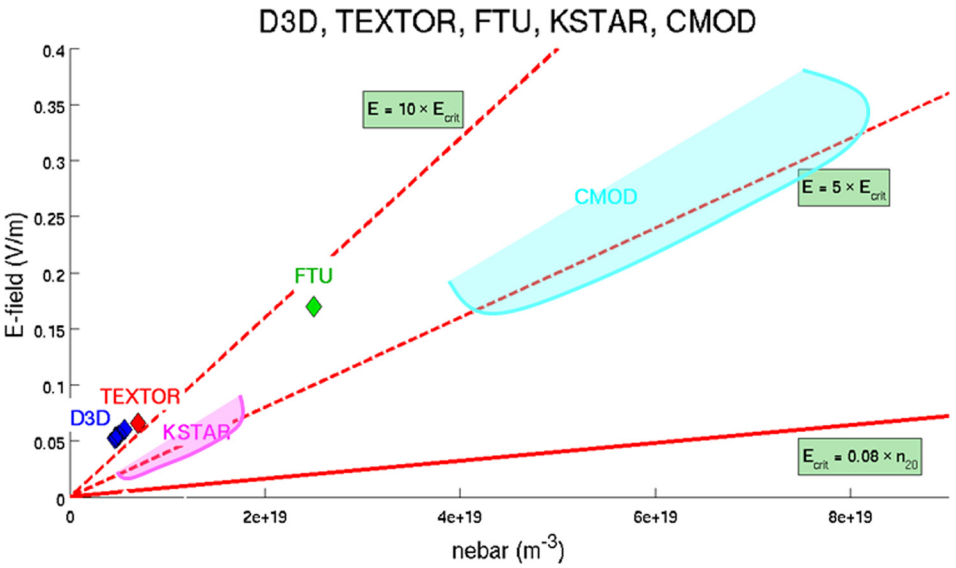

FIG. 8. Compilation of RE detection threshold data from all contributors to date in the joint ITPA study. These data suggest that other RE loss mechanisms dominate over collisional drag, even during the quiescent flattops of discharges.

become important. In the avalanche process, a runaway electron has a Coulomb collision with a background thermal electron, imparting enough forward momentum to kick the thermal electron to runaway energies, while still leaving itself at runaway energies. Both of these runaways then continue to accelerate and collide with thermal background electrons to create even more runaways. This secondary, or avalanche, mechanism is therefore an exponential process, with a growth rate, $\gamma_{\rm sec}$, given by Eq. (18) in Ref. 1, and which scales like:

$$\gamma_{\rm sec} \propto \left(\frac{E}{E_{\rm crit}} - 1\right), \tag{7}$$

where $E_{\rm crit}$ is the Connor-Hastie threshold E-field (Eq. (5)). Thus, the total growth rate of the RE population, *in the absence of any loss mechanisms other than Coulomb collisions*, is the sum of the primary (linear) and secondary (exponential) processes:

$$\frac{dn_{\rm RE}}{dt} = \left(\frac{dn_{\rm RE}}{dt}\right)^{\rm primary} + \gamma_{\rm sec} n_{\rm RE}. \tag{8}$$

The initial RE production is via the primary mechanism, but the secondary process will eventually dominate due to its exponential nature if the plasma flattop duration is sufficiently long.

D. Experimental measurements of RE growth and decay rates

The plasma parameters relevant for RE growth ($n_{\rm e}$, $V_{\rm loop}$, $T_{\rm e}$, $Z_{\rm eff}$) can be measured during the quiescent flattop, so one way of comparing the empirical threshold field to $E_{\rm crit}$ is to evaluate Eq. (8) based on the measured plasma parameters and compare to the measured RE evolution. This could even be done in a least squares sense, treating $E_{\rm crit}$ as a free parameter, so that it can be directly compared to the Connor-Hastie value. However, this requires at least a relative calibration of the RE diagnostic, i.e., knowledge of the correspondence between the HXR or synchrotron measurement and the RE population. As mentioned previously, this knowledge is lacking in present experiments. A simpler method, which bypasses this issue, is possible once the RE dynamics are dominated by the secondary mechanism. In this case, $n_{\rm RE}(t)$ will be purely exponential, so ln $n_{\rm RE}(t)$ can be fit with a straight line whose slope is $\gamma_{\rm sec}$. If the plasma conditions are above the RE threshold, the RE population will be growing, and the growth rate will be positive, $\gamma_{\rm sec} > 0$. If the plasma conditions are below the RE threshold, the RE population will be decaying, and the growth rate will be negative, $\gamma_{\rm sec} < 0$. From Eq. (7), it is seen that the transition between positive and negative γ should occur at $E/E_{\rm crit} = 1$. Detailed knowledge of the RE diagnostic calibration is therefore not necessary; the crucial information is simply whether the signal is increasing or decreasing for a given $E/E_{\rm crit}$.

An experiment to do this was performed on DIII-D, and signals from a subset of the shots are shown in Figure 9. The density during the early part of each discharge decreases slowly, resulting in the formation of an RE population, as

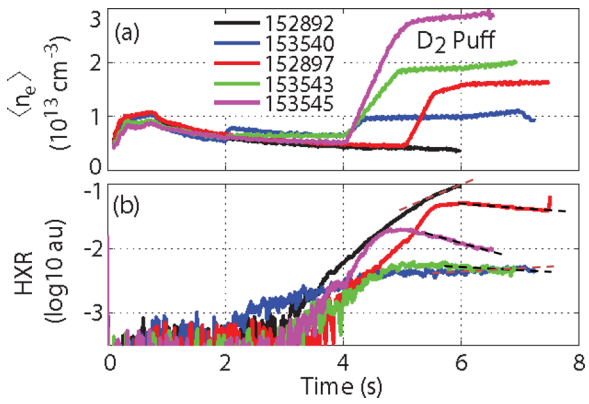

FIG. 9. DIII-D measurements of density and log(HXR) on 5 shots are shown, with linear fits (dashed lines) to determine growth and decay rates. Low densities early in the discharges promote RE growth. Densities are increased later in the discharges to suppress the runaways. (Adapted with permission from Ref. 6; copyright 2014 American Institute of Physics.)

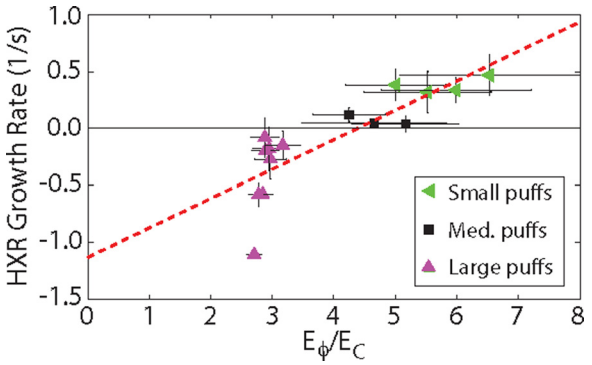

FIG. 10. RE growth rates measured on DIII-D transition from positive values to negative values (i.e., decay) at $E/E_{crit} = 3$–5 (dashed line). Collisional theory predicts that the transition should occur at $E/E_{crit} = 1$. These results imply that other RE loss mechanism are playing a role. (Adapted with permission from Ref. 6; copyright 2014 American Institute of Physics.)

seen on the hard x-ray diagnostic. On some of the discharges the density is then increased relatively quickly, and then plateaued at a higher level, still during the I_p flattop. The log of the HXR signals is well fitted by straight lines, indicating that the signals are exponential and therefore governed by Eq. (7). On the three highest density discharges (corresponding to low E/E_{crit}), the RE signals decrease during the latter portion of the discharges, which corresponds to negative growth rates. Analyses of a dedicated set of discharges on DIII-D covering a range of E/E_{crit} values has been done,[6] and the results are plotted in Figure 10. The measured γ's transition from positive (growth) to negative (decay) values at $E/E_{crit} = 3$–5. Collisional theory, however, predicts that the transition between growth and decay should occur at $E/E_{crit} = 1$, as construed in Eq. (7). Hence, this method of determining the RE threshold conditions leads to a similar conclusion as obtained with the detection onset method, namely that the E-field must be at least 3–5 times higher than E_{crit} in order to get RE generation, or conversely, runaways can be mitigated at densities 3–5 times less than predicted for collisional-only damping.

IV. SUMMARY AND DISCUSSION

The RE threshold results determined from the growth/decay method and possibly the detection onset method imply that there are other RE loss mechanisms in addition to collisional damping, and that these additional loss mechanisms may dominate, even during the quiescent I_p flattop. The ITPA joint experiment will continue for the near future, both to add data from additional machines, and to investigate the nature of the additional loss mechanism(s). The results could have important implications for mitigating runaways on ITER, assuming: (1) they apply even though ITER is significantly larger than the machines that have contributed data so far, and (2) they apply during disruptions, not just during the quiescent I_p flattop. There are a number of non-collisional RE loss mechanisms that can be invoked, such as synchrotron radiation from Larmor motion (which requires a mechanism to pitch angle scatter some fraction of the parallel runaway energy), or large magnetic fluctuations (either stochastic or low m,n) which might cause spatial diffusive loss of runaways. These effects are likely to be even more prevalent during disruptions than during the quiescent flattop. However, it should be noted that substantial synchrotron losses first require that runaways be generated and then accelerated to highly relativistic energies, which seems to preclude any effect on the RE threshold, when runaways are first forming. The results of this joint experiment provide an excellent opportunity for focused theoretical and modeling efforts to understand the additional RE loss mechanisms during the quiescent flattop, and the implications for RE plateau formation and RE losses during disruptions, which has been studied in DIII-D (Refs. 7 and 8) and elsewhere.

V. DISCLAIMER

The views and opinions expressed herein do not necessarily reflect those of the ITER Organization.

ACKNOWLEDGMENTS

This work supported in part by: US Department of Energy under DE-FC02-99ER54512-CMOD, DE-FC02-04ER54698 (GA), and DE-AC05-06OR23100 (ORISE).

Korea Ministry of Science, ICT and Future Planning under the KSTAR project.

Direccion General de Investigacion, Cientifica y Tecnica (Ministerio de Economia y Competitividad), Project No. ENE2012-31753.

The authors wish to thank the experimental teams of DIII-D, C-Mod, FTU, KSTAR, and TEXTOR for their support in performing the experiments and contributing the data.

One of the authors (H. R. Koslowski) wishes to acknowledge the assistance of K. Wongrach, Univ. of Dusseldorf, Germany in analyzing the TEXTOR IR data.

[1]M. N. Rosenbluth and S. V. Putvinski, Nucl. Fusion **37**, 1355–1362 (1997).
[2]J. W. Connor and R. J. Hastie, Nucl. Fusion **15**, 415–424 (1975).
[3]H. Dreicer, Phys. Rev. **117**, 329–342 (1960).
[4]T. C. Hender, J. C. Wesley, J. Bialek, A. Bondeson, A. H. Boozer, R. J. Buttery, A. Garofalo, T. P. Goodman, R. S. Granetz, Y. Gribov, O. Gruber, M. Gryaznevich, G. Giruzzi, S. Günter, N. Hayashi, P. Helander, C. C. Hegna, D. F. Howell, D. A. Humphreys, G. T. A. Huysmans, A. W. Hyatt, A. Isayama, S. C. Jardin, Y. Kawano, A. Kellman, C. Kessel, H. R. Koslowski, R. J. La Haye, E. Lazzaro, Y. Q. Liu, V. Lukash, J. Manickam, S. Medvedev, V. Mertens, S. V. Mirnov, Y. Nakamura, G. Navratil, M. Okabayashi, T. Ozeki, R. Paccagnella, G. Pautasso, F. Porcelli, V. D. Pustovitov, V. Riccardo, M. Sato, O. Sauter, M. J. Schaffer, M. Shimada, P. Sonato, E. J. Strait, M. Sugihara, M. Takechi, A. D. Turnbull, E. Westerhof, D. G. Whyte, R. Yoshino, and H. Zohm, Nucl. Fusion **47**, S128 (2007).
[5]J. R. Martin-Solis, R. Sánchez, and B. Esposito, PRL **105**, 185002 (2010).
[6]C. Paz-Soldan, N. W. Eidietis, R. S. Granetz, E. M. Hollmann, R. A. Moyer, J. C. Wesley, J. Zhang, M. E. Austin, N. A. Crocker, A. Wingen, and Y. Zhu, Phys. Plasmas **21**, 022514 (2014).
[7]E. M. Hollmann, N. Commaux, N. W. Eidietis, T. E. Evans, D. A. Humphreys, A. N. James, T. C. Jernigan, P. B. Parks, E. J. Strait, J. C. Wesley, J. H. Yu, M. E. Austin, L. R. Baylor, N. H. Brooks, V. A. Izzo, G. L. Jackson, M. A. Van Zeeland, and W. Su, Phys. Plasmas **17**, 056117 (2010).
[8]E. M. Hollmann, M. E. Austin, J. A. Boedo, N. H. Brooks, N. Commaux, N. W. Eidietis, D. A. Humphreys, V. A. Izzo, A. N. James, T. C. Jernigan, A. Loarte, J. Martin-Solis, R. A. Moyer, J. M. Muñoz-Burgos, P. B. Parks, D. L. Rudakov, E. J. Strait, C. Tsui, M. A. Van Zeeland, J. C. Wesley, and J. H. Yu, Nucl. Fusion **53**, 083004 (2013).